J Appl Physiol 112: 204–211, 2012.
First published September 29, 2011; doi:10.1152/japplphysiol.00953.2011.

Microparticle enlargement and altered surface proteins after air decompression are associated with inflammatory vascular injuries

Ming Yang,[1] Tatyana N. Milovanova,[1] Marina Bogush,[1] Günalp Uzun,[3] Veena M. Bhopale,[1] and Stephen R. Thom[1,2]

[1]*Institute for Environmental Medicine and* [2]*Department of Emergency Medicine, University of Pennsylvania Medical Center, Philadelphia, Pennsylvania; and* [3]*Department of Underwater and Hyperbaric Medicine, Gulhane Military Medical Academy, Haydarpasa Teaching Hospital, Uskudar, Istanbul, Turkey*

Submitted 28 July 2011; accepted in final form 27 September 2011

Yang M, Milovanova TN, Bogush M, Uzun G, Bhopale VM, Thom SR. Microparticle enlargement and altered surface proteins after air decompression are associated with inflammatory vascular injuries. *J Appl Physiol* 112: 204–211, 2012. First published September 29, 2011; doi:10.1152/japplphysiol.00953.2011.—Studies in a murine model have shown that decompression stress triggers a progressive elevation in the number of circulating annexin V-coated microparticles derived from leukocytes, erythrocytes, platelets, and endothelial cells. We noted that some particles appeared to be larger than anticipated, and size continued to increase for ≥24 h postdecompression. These observations led to the hypothesis that inert gas bubbles caused the enlargement and particle size could be reduced by hydrostatic pressure. After demonstrating pressure-induced particle size reduction, we hypothesized that annexin V-positive particle changes associated with decompression contributed to their proinflammatory potential. Intravenous injection of naive mice with particles isolated from decompressed mice, but not control mice, caused intravascular neutrophil activation; perivascular neutrophil sequestration and tissue injuries were documented as elevations of vascular permeability and activated caspase-3. These changes were not observed if mice were injected with particles that had been subjected to hydrostatic recompression or particles that had been emulsified by incubation with polyethylene glycol telomere B surfactant. Hydrostatic pressure and surfactant incubation also altered the pattern of proteins expressed on the surface of particles. We conclude that proinflammatory events and vascular damage are due to enlargement of annexin V-coated particles and/or changes in surface marker protein pattern associated with provocative decompression. Injection of annexin V-coated particles from decompressed mice will recapitulate the pathophysiological vascular changes observed following decompression stress.

decompression sickness; intravascular bubble; leukocytes; platelets; antigen sharing; CD41; integrins; myeloperoxidase

DECOMPRESSION SICKNESS (DCS) is a systemic pathophysiological process that occurs after tissues become supersaturated with gas. Inert gases inhaled while breathing are taken up by tissues in proportion to the ambient pressure, and when pressure is reduced, some of the gas released from tissues forms bubbles because of the presence of gas cavitation nuclei (4, 7, 25, 26). The central role of bubbles as an inciting factor for DCS is widely accepted, but the pathophysiological responses that mediate tissue injury remain unclear. DCS has been associated with endothelial dysfunction, platelet activation, occasional alterations in coagulation pathways, and rare reduction of circulating platelet counts (2, 18–20). Neutrophil activation and perivascular adherence are associated with functional deficits postdecompression in animal models (14, 17). DCS is a risk associated with deep-sea SCUBA diving, high-altitude aviation, and space exploration.

Microparticles (MPs) are defined as 0.1- to 1.0-μm-diameter lipid bilayer-enclosed membranous vesicles. MPs are generated when cells undergo oxidative stress, apoptosis, or cell activation/calcium influx, and circulating MPs are characterized by their expression of antigenic markers from parent cells (5, 6, 8, 21). As MPs bud from these cells, negatively charged phosphatidylserine residues are exposed, which often leads to secondary binding of annexin V. MPs can directly stimulate release of proinflammatory cytokines, and platelet-derived MPs stimulate leukocyte activation and aggregation (10, 12, 15). Annexin V-positive platelet MPs exhibit procoagulant activity (3).

Circulating MPs are increased in humans subjected to simulated SCUBA diving (13, 24). We have reported that mice subjected to varying decompression stresses exhibit progressive elevations in circulating MPs derived from leukocytes, erythrocytes, platelets, and endothelial cells (23). We showed that MPs can be lysed by incubation with a surfactant, polyethylene glycol telomere B (PEG). The number of circulating MPs in mice subjected to decompression stress can be reduced by infusion with PEG or with antibody to annexin V. These manipulations will reduce decompression-induced intravascular neutrophil activation, perivascular neutrophil sequestration, and tissue injury documented as elevations of vascular permeability and activated caspase-3.

While observing MPs from decompressed mice, we noted that some appeared to be larger than anticipated. We hypothesized that particle enlargement might arise because of inert gas supersaturation associated with decompression, and size could be reduced if the particles were exposed to hydrostatic pressure. Furthermore, we hypothesized that changes in MPs associated with decompression contributed to their proinflammatory potential. Therefore, additional studies were conducted to evaluate annexin V-positive particle surface markers and the propensity for annexin V-positive particles to elicit neutrophil activation and vascular damage when injected into naive mice.

METHODS

Materials. Unless otherwise noted, chemicals were purchased from Sigma-Aldrich (St. Louis, MO). Annexin binding buffer and the following antibodies were purchased from BD Pharmingen (San Jose, CA): FITC-conjugated anti-annexin V, FITC-conjugated anti-mouse myeloperoxidase (MPO), R-phycoerythrin (R-PE)-conjugated anti-

Address for reprint requests and other correspondence: S. R. Thom, Institute for Environmental Medicine, Univ. of Pennsylvania, 1 John Morgan Bldg., 3620 Hamilton Walk, Philadelphia, PA 19104-6068 (e-mail: sthom@mail.med.upenn.edu).

mouse CD146, PerCP/Cy5.5-conjugated anti-mouse CD41, PerCP/Cy5.5-conjugated anti-mouse CD14, allophycocyanin (APC)-conjugated anti-mouse glycophorin A, APC-conjugated anti-mouse CD31, and APC-conjugated anti-mouse von Willebrand factor. R-PE-conjugated anti-mouse CD41 was purchased from e-Biosciences (San Diego, CA), PerCP/Cy5.5-conjugated anti-human CD66b from Biolegend (San Diego, CA), and Alexa 647-conjugated anti-mouse CD18 from Serotec (Raleigh, NC).

Animals. All aspects of the study were reviewed and approved by the Institutional Animal Care and Use Committee. Mice (*Mus musculus)* were purchased from Jackson Laboratories (Bar Harbor, ME), fed a standard rodent diet and water ad libitum, and housed in the animal facility of the University of Pennsylvania. Mice were left to breathe room air (control) or subjected to 790 kPa (100 psi) air pressure for 2 h as described elsewhere (23). All manipulations were as described previously (23), except only a small aliquot of heparinized blood obtained from anesthetized mice was immediately combined with commercial fixative (100 μl/ml Caltag Reagent A fixation medium, Invitrogen, Carlsbad, CA) after decompression for evaluation of leukocyte activation and MPs. Most blood was not fixed immediately, because immediate fixation of blood prevented postdecompression changes in the size of the MPs.

Standard procedures for MP acquisition and processing. All reagents and solutions used for MP analysis were sterile and filtered (0.2-μm filter). Most of the blood used in the study was obtained from mice killed 2 h after exposure to 790 kPa air pressure for 2 h. Blood samples from two mice were typically pooled to obtain sufficient material for daily experiments. Heparinized blood was centrifuged for 5 min at 1,500 *g*, and the supernatant was suspended in 0.2 M EDTA to diminish ex vivo MPs aggregation. Some of the sample was fixed and used to analyze MP sizes in early experiments. In the majority of studies, the supernatant was centrifuged at 15,000 *g* for 30 min to pellet the few remaining platelets and cell debris. Supernatant was parceled among centrifuge tubes at a ratio of 250 μl to 4 ml of PBS and centrifuged at 100,000 *g* for 60 min (typically 3–4 tubes/experiment). Supernatant (4 ml) was then carefully removed, and a small portion was analyzed to assess MP isolation efficiency. The supernatant solutions remaining after the 100,000-*g* centrifugation of control samples contained 252 ± 25 (SE) MPs/μl, and samples from decompressed mice contained 256 ± 31 MPs/μl [$n = 11$, $P =$ not significant (NS)]. We conclude that MP recovery efficiency did not differ between samples. The MP pellet was resuspended in the ~250 μl of supernatant remaining in the centrifuge tube and used for further experimentation.

The resuspended MP samples were combined at a 1:1 (vol/vol) ratio with PBS, and aliquots were placed in sterile syringes. All MP samples for daily experiments were pooled and processed to generate one of three suspensions (*type a, b*, or *c*) for injection into naive mice. *Type a* particles were left on the benchtop for 1 h, *type b* particles were subjected to hydrostatic recompression to 790 kPa and incubated for 1 h at room temperature, and *type c* particles were made 33% (vol/vol) with PEG and incubated at 37°C for 1 h to lyse the annexin V-positive particles. To achieve hydrostatic recompression, the samples contained within closed plastic syringes were placed inside a stainless steel pressure vessel with 1.4-cm-thick walls and 260-ml internal volume. Air pressure was applied, so that the syringe plunger subjected the MP solution to an elevated hydrostatic pressure. Temperature changes associated with this process were determined with a thermometer immersed in the same volume of solution used in MP experiments. No measurable change in temperature (sensitivity limit 0.1°C) was noted, which we interpret as due to the large heat sink posed by the thick steel chamber walls.

After these incubations, a small portion of the sample was fixed [1:10 (vol/vol) with Caltag fixative] to count and characterize the particles. Aliquots of *type a* or *b* particles (200 μl) were combined with 200 μl of PBS and placed in new sterile syringes for intravenous injections. Aliquots of *type c* particles (200 μl of particles had been combined with 100 μl of PEG for the 1-h incubation) were combined with 100 μl of PBS. At exactly 2 h following isolation of annexin V-positive particles from mice by the 15,000 *g* centrifugation, 400-μl preparations of one of the three particle samples were injected into naive mice via the dorsal tail vein. Control animals were injected with 400 μl of PBS; as a control for the PEG-incubated particle studies, mice were injected with 400 μl of a 25% (vol/vol) solution of PEG in PBS. At 1 h after injection, mice were anesthetized, exsanguinated, and injected with lysine-fixable rhodamine-dextran (2×10^6 Da) and then with colloidal silica following published methods (23). Endothelium-enriched fractions were obtained for analysis from brain, leg skeletal muscle, psoas, and omentum.

Flow cytometry. Flow cytometry was performed with a 10-color FACSCanto (Becton Dickinson, San Jose, CA) using standard acquisition software. Events were counted based on light scatter, with gates set to include 0.3- to 6.5-μm particles, excluding background corresponding to debris usually present in buffers. MPs were stained with annexin V antibody and analyzed as previously described, except samples also included 0.3-μm-diameter (Sigma) and 1.0-, 3.0-, and 6.5-μm-diameter (Spherotech, Lake Forest, IL) microbeads, which were used for initial settings and before each experiment to estimate MP diameters. Analysis involved establishing true-negative controls by a fluorescence-minus-one analysis and by using isotype-matched irrelevant antibodies at the same concentration and under the same conditions. Forward and side scatter were set at logarithmic gain. The absolute numbers of MPs per milliliter of plasma were determined by counting the proportion of beads and the exact volume of plasma from which MPs were analyzed. Analysis of leukocytes was performed on fixed blood samples, as previously described (23).

Colloidal silica-endothelium isolation technique and Western analysis. Methods were exactly as described elsewhere (23). Tissue supernatants prepared from brain, omentum, leg skeletal muscle, and psoas were analyzed by Western blots, with β-actin used to control for protein loading.

Vascular permeability assay. Lysine-fixable tetramethylrhodamine-conjugated dextran (2×10^6 Da; Invitrogen) was prepared and used exactly as described elsewhere (23). Vascular permeability, quantified as perivascular dextran uptake in experimental groups, was normalized to a value obtained with a control mouse included in each experiment.

Confocal microscopy. Images of annexin V-positive particles were acquired using a Zeiss Meta510 confocal microscope equipped with a Plan-Apochromat ×63/1.4 numerical aperture oil objective, as previously described (23). Particle suspensions were stained with R-PE-conjugated anti-annexin V antibody, as previously described (23), combined with a small number of FITC-containing 0.86-μm-diameter beads (Sigma), and placed on slides. Slides were visually inspected to ensure that no aggregates were present; then images were obtained and analyzed using ImageJ software.

Statistical analysis. Sigmastat software (Systat, Point Richmond, CA) was used for statistical analysis. Neutrophil activation, elevations in size of different circulating annexin V-positive particle populations, and tissue changes across multiple organs were analyzed by ANOVA followed by the Holm-Sidak test. Single comparisons were performed using Student's *t*-tests.

RESULTS

MP elevations postdecompression. This investigation focused on changes in MPs from mice after they were decompressed following exposure to 790 kPa air pressure for 2 h. As in previous studies, the number of circulating MPs was elevated after decompression. Control animals (~100 kPa air pressure) had 1,982 ± 145 (SE) MPs/μl plasma ($n = 11$). At 2 h after decompression, mice had 8,165 ± 402 ($P < 0.05$, $n = 11$) MPs/μl plasma. Among all ≤1-μm-diameter circulating

particles, 97.4 ± 0.5% were annexin V-positive in control mice and 95.4 ± 0.5% (P = NS) were annexin V-positive in mice killed 2 h after the decompression stress.

MPs enlarge after decompression. The morphology of annexin V-positive MPs was examined using a multi-photon microscope. FITC-containing 0.86-μm-diameter beads were included in the suspensions to estimate particle sizes. In most microscope fields of samples from mice subjected to decompression stress, many annexin V-positive particles appeared to be larger than the FITC-beads (Fig. 1). To survey a large number of particles, blood was obtained for flow cytometry analysis from control mice exposed to ambient air or from mice exposed to 790 kPa air pressure for 2 h and then left undisturbed for up to 24 h before they were killed. Blood was fixed immediately after it was obtained from the mice. As shown in Fig. 2, virtually all annexin V-positive particles from control mice were 0.3–1 μm. At various times postdecompression, however, the 0.3- to 1-μm pool size was significantly diminished and a greater proportion of annexin V-positive particles exceeded this size range.

While measures were taken to avoid MP aggregation in the plasma samples, we were concerned that what appeared to be enlarged annexin V-positive particles in the flow cytometer might be MP aggregates. Therefore, a new series of studies was performed. Mice were subjected to decompression, blood samples were fixed, and after annexin V-positive particles were isolated, the particles were inspected by confocal microscopy. Once we were assured that there were no particle aggregates, particle diameters were evaluated using computer imaging software. The distribution of annexin V-positive particles is shown in Table 1. There were significantly higher percentages with diameters >1.0 μm in samples from decompressed mice. In control mice, 5.5% of annexin V-positive particles were >1.0 μm. The mean diameter of these larger particles was 1.44 ± 0.03 μm (n = 5). In mice killed immediately after decompression, 16.4% of annexin V-positive particles were >1.0 μm ($P < 0.05$ vs. control), and the mean diameter of the larger particles was 1.44 ± 0.04 μm (n = 6, P = NS vs. control). In mice killed 2 h postdecompression, 22.9% of annexin V-positive particles were >1.0 μm ($P < 0.05$ vs. control and immediate postdecompression mice), and the mean diameter of these particles was 2.87 ± 0.63 μm (n = 5, $P < 0.05$ vs. control and immediate postdecompression mice). In mice killed 24 h postdecompression, 18.6% of annexin V-positive particles were >1.0 μm ($P < 0.05$ vs. control and immediate postdecompression mice), and the mean diameter of these larger particles was 3.31 ± 0.80 μm (n = 3, $P < 0.05$ vs. control and immediate postdecompression mice).

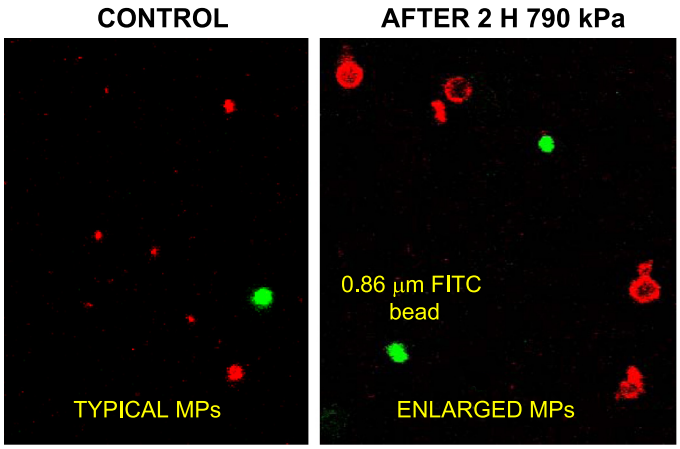

Fig. 1. Confocal microscopy images of annexin V-positive microparticles (MPs). Image frames include 0.86-μm-diameter green fluorescent (FITC) beads. Samples prepared from decompressed mice exhibited numerous annexin V-positive particles that appeared to have diameters >1 μm.

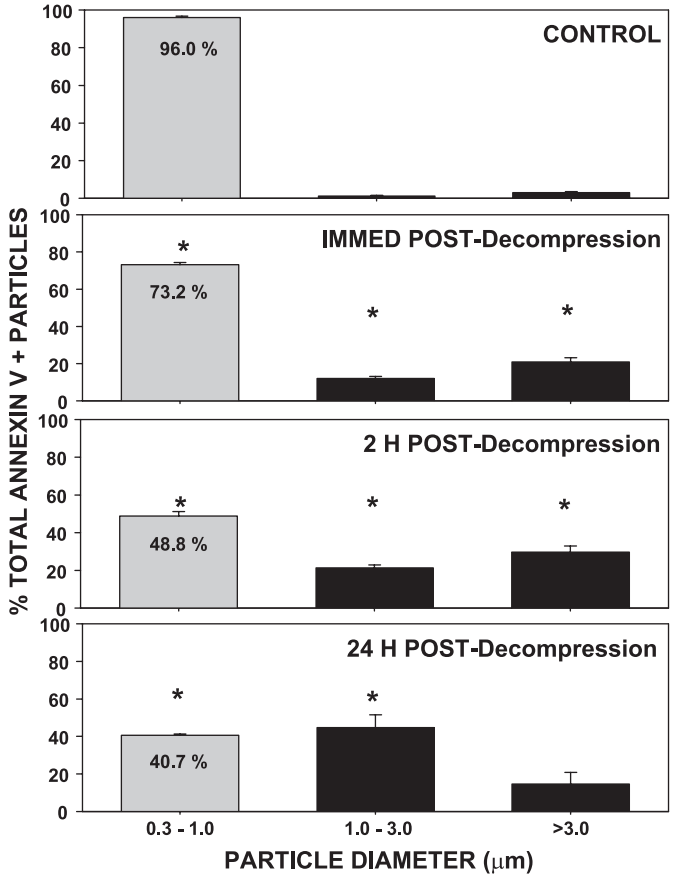

Fig. 2. Flow cytometric analysis of size distribution of blood-borne annexin V-positive particles postdecompression. Blood from control mice and mice exposed to 790 kPa air pressure for 2 h was fixed immediately after it was withdrawn to prevent MP enlargement. Analysis was based on comparison of annexin V-positive particles with fluorescent beads added to each suspension prior to analysis. Values are means ± SE; n = 3–4 in all groups. *$P < 0.05$ vs. control.

Large MPs can be reduced in size by hydrostatic recompression. We hypothesized that annexin V-positive particle enlargement postdecompression may occur because of the presence of inert gas bubbles. To test this, samples were subjected to hydrostatic pressure. As described in METHODS, for these studies, particle samples were obtained from mice killed 2 h after exposure to 790 kPa air pressure for 2 h. Analyses of particle sizes in samples exposed for 1 h to ambient pressure or to 790 kPa hydrostatic pressure are shown in Table 2. It was clear that hydrostatic recompression reduced the fraction of >1-μm-diameter particles. With this finding, our plan was to evaluate the pathophysiological impact of injecting the annexin V-positive particles into normal mice.

Leukocyte activation caused by particle injections. Plasma particles were isolated from decompressed mice and processed

Table 1. *Size distribution of annexin V-positive particles*

Decompression Status	*n*	Diameter				
		0.1–0.5 μm	0.5–1.0 μm	1.0–1.5 μm	1.5–2.0 μm	>2.0 μm
Control	5	47.6 ± 5.4	46.9 ± 4.8	4.1 ± 0.6	0.8 ± 0.1	0.6 ± 0.1
Immediately postdecompression	5	42.3 ± 5.4	41.3 ± 5.4	11.4 ± 0.9*	4.1 ± 1.2*	0.9 ± 0.1
2 h postdecompression	5	43.3 ± 4.2	33.8 ± 2.6	6.5 ± 0.9	6.6 ± 2.3*	9.8 ± 1.8*
24 h postdecompression	3	57.4 ± 4.5	24.0 ± 1.2*	2.7 ± 0.9*	1.3 ± 1.0	14.6 ± 4.9*

Values are means ± SE, expressed as percentage of total; *n*, number of animals. Number of particles analyzed from each mouse averaged 1,343 (range 555–3,885). Plasma samples were obtained from control mice or mice exposed to 790 kPa air pressure for 2 h and killed immediately, 2 h, or 24 h later. Blood was fixed immediately after it was withdrawn from the mice to prevent ex vivo particle enlargement. Diameters were quantified using computer imaging software. *$P < 0.05$.

as described in METHODS for intravenous injection into naive mice. After isolation, samples were manipulated for 1 h in one of three ways: (*a*) left on the benchtop (no recompression), (*b*) subjected to hydrostatic recompression, or (*c*) incubated with PEG to cause particle lysis. The mean number of annexin V-positive particles in these samples after manipulations and prior to injection into normal mice is shown in Table 3. All samples were injected exactly 2 h after isolation from plasma.

Figure 3 shows a series of measurements of neutrophils obtained from mice injected with one of the five solutions: *type a, b*, or *c* plasma sample, PBS (control), or the same concentration of PEG in PBS that matched the *type c* plasma samples. The only neutrophils to exhibit evidence of activation based on significantly increased surface expression of CD18 (a component of β_2-integrins), MPO, and also evidence of interaction with platelets or platelet-derived particles based on surface expression of CD41, the platelet-specific α_{2b}-integrin protein, were those from mice injected with *type a* particles.

Perivascular changes caused by particle injections. Next, we examined whether injecting the different types of annexin V-positive particles caused perivascular changes similar to those we have reported for decompressed mice. Tissue homogenates from brain, omentum, leg muscle, and psoas were enriched for vascular endothelium. Significant elevations of the neutrophil-specific CD66b protein, MPO, and cleaved caspase-3 were found in mice injected with *type a* particles but not in mice injected with any of the other solutions (Fig. 4).

Increased vascular permeability caused by plasma particle injections. Vascular permeability to rhodamine-labeled dextran was assayed in the same mice used for the analyses of perivascular protein deposition. Permeability to lysine-fixable 2×10^6 Da rhodamine-conjugated dextran was significantly elevated in all tissues from mice injected with *type a* plasma particles, but no significant leak was detected in mice injected with the other solutions (Fig. 5).

Annexin V-positive particles in the circulation of injected mice. We have shown that decompression stress increases the number of circulating MPs and that these MPs interact such that they express numerous markers for different cell types. We were interested in analyzing the circulating MPs in mice injected with the various solutions (PBS, PBS + PEG, and *type a, b*, and *c* particles). No significant elevations in particle numbers were found among mice injected with PEG-containing solutions (Fig. 6). There were significantly more MPs in mice injected with *type a* and *b* particles than in control (PBS-injected) mice. The number of MPs was significantly higher in the mice injected with particles left at ambient pressure (*type a*) than in those subjected to hydrostatic recompression (*type b*).

Subtype analysis of the circulating MPs is shown in Fig. 7. MPs expressing each protein were significantly elevated over control in mice injected with standard or recompressed annexin V-positive particles (*type a* or *b* suspensions). As in our prior report, because some MPs express more than one surface protein, the total for a mouse group may exceed 100%. Although values appear somewhat higher in mice injected with particle samples preincubated with PEG, these values were not significantly elevated over values in mice injected with PBS or PBS + PEG (ANOVA).

Surface markers on injected MPs. The differences in circulating MPs from mice injected with the different preparations prompted us to examine the surface protein expression patterns for the annexin V-positive particle samples prepared for injection. That is, samples were analyzed by flow cytometry before they were injected into mice. Hydrostatic pressurization and PEG incubation caused significant changes in surface proteins compared with samples left for 1 h in PBS at ambient pressure (Table 4).

DISCUSSION

MPs have been implicated in a number of pathological processes, and we have demonstrated their involvement with proinflammatory injuries following decompression stress (6, 8, 23). Results from this study demonstrate that intravascular phenomena associated with MPs are complex, and injuries

Table 2. *Change in particle size distribution by hydrostatic recompression*

Treatment	Diameter				
	0.1 to 0.5 μm	0.5 to 1.0 μm	1.0–1.5 μm	1.5–2.0 μm	>2.0 μm
Ambient pressure	49.1 ± 0.7 (6)	36.9 ± 0.5 (6)	5.2 ± 0.9 (6)	1.9 ± 0.7 (6)	6.9 ± 1.9 (6)
Hydrostatic recompression	48.5 ± 0.3 (5)	47.6 ± 0.3 (5)	2.6 ± 0.2* (5)	0.7 ± 0.1* (5)	0.6 ± 0.3* (5)

Values are means ± SE, expressed as percentage of total number of annexin V-positive particles; number of animals is shown in parentheses. Samples were obtained from mice exposed to 790 kPa air pressure for 2 h and then exposed to ambient pressure or 790 kPa hydrostatic pressure for 1 h. Analyses were performed on samples fixed exactly 2 h after being obtained from mice. *$P < 0.05$.

Table 3. *Annexin V-positive particles in injected preparations*

Preparation	Number of Particles
Benchtop	30,790 ± 1,536 (17)
Hydrostatic pressure	42,119 ± 4,358 (11)
PEG incubation	2,711 ± 599* (6)

Values are means ± SE, expressed as number of particles per microliter of solution; number of animals is shown in parentheses. 200 μl of particles were injected into each mouse. PEG, polyethylene glycol telomere B. *$P < 0.05$ vs. the other 2 samples.

linked to their presence involve more than merely an increase in the number of circulating MPs.

Annexin V-positive particle size. Early in this study, we found that annexin V-positive particles enlarge postdecompression, and sizes continue to change for ≥24 h. We evaluated this issue using flow cytometry and microscopy. We believe the microscopic measurements are more reliable, because there is greater sensitivity to detect small differences in particle sizes via microscopic measurement than via flow cytometry and there is greater assurance that particle aggregates are not being measured.

Particle sizes can be reduced by hydrostatic recompression, indicating that some contain a gas phase. Several potential mechanisms explain this process. Some particles normally have a gas nucleus; so on decompression, nitrogen from supersaturated tissues diffuses into the gas phase to cause particle enlargement. This is an appealing possibility, because the size of the particles fits mathematical models predicting the size of gas cavitation nuclei in previous studies of decompression pathophysiology. Gas nuclei responsible for inert gas bubble formation were predicted to have a radius up to ~0.6 μm (e.g., 1.2 μm diameter) (7, 25, 26). Of course, how MPs should come to have a gas phase is unknown.

An alternative mechanism is that gas bubbles form on decompression, and existing MPs in the circulation are disrupted by bubble shear forces. The proteins and lipids that comprise the MPs then reaggregate around the gas bubbles, which are the source of the enlarged, annexin V-positive particles observed in the plasma of decompressed mice. A fragmentation event might also explain why the number of particles in recompressed samples (*type b*) tended to be higher. While the number of *type b* particles injected was not statistically significantly different from the number of *type a* particles, on average ~12,000 more particles/μl were present in samples consisting of *type b* particles (Table 3).

Annexin V-positive particle surface proteins. Manipulations to prepare MPs for injection that involved hydrostatic pressure and PEG incubation (*type b* and *c*) altered their surface protein expression patterns (Table 4). The surface marker pattern of MPs isolated from decompressed mice and left on the benchtop for 1 h to generate standard (*type a*) suspensions is very similar to the pattern seen on MPs directly isolated from mice subjected to decompression from 790 kPa, as we reported previously (23). We conclude, therefore, that merely incubating particle suspensions in PBS for 1 h causes little change in surface marker distribution. This contrasts sharply with surface marker patterns observed on particles subjected to hydrostatic pressure (*type b*) or PEG incubation (*type c*). That emulsification with PEG should cause surface marker redistribution is not particularly surprising. We believe that evidence of redistribution of surface proteins caused by subjecting particles to hydrostatic pressure offers indirect evidence that some, indeed,

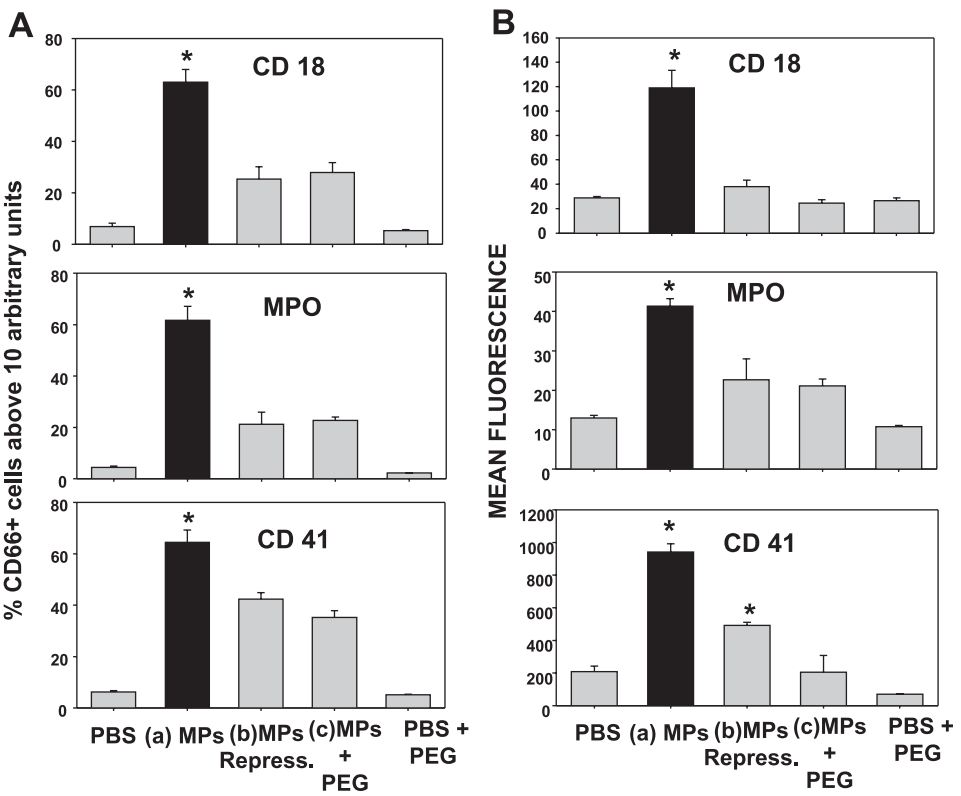

Fig. 3. Neutrophil activation due to MP injections. Neutrophils were identified by CD66b staining, and coexpression of CD18, myeloperoxidase (MPO), and CD41 was assessed by flow cytometry. *A*: percentage of CD66b-positive cells expressing a geometric mean fluorescence value ≥10 arbitrary fluorescence units for each surface marker. *B*: CD66b-positive cell geometric mean fluorescence for each marker. PBS, injections of sterile saline only; MPs, annexin V-positive particles isolated from decompressed mice and left on the benchtop for 1 h at ambient pressure; MPs Repress, MPs subjected to hydrostatic recompression for 1 h; PEG + MPs, MPs incubated with polyethylene glycol telomere B (PEG); PBS + PEG, injection with PBS containing PEG but no MPs. Values are means ± SE; $n = 4$–10 per group. *$P < 0.05$ vs. control.

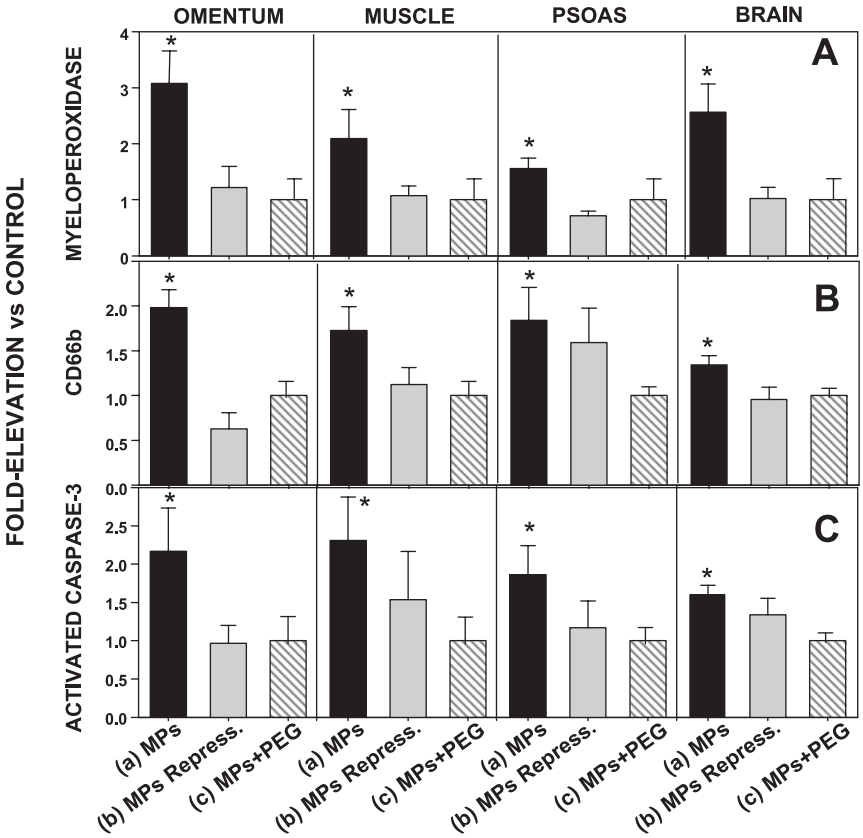

Fig. 4. MPO, CD66b, and activated caspase-3 in tissue homogenates. Tissues were isolated, enriched for endothelium, and analyzed. Western blot band densities are expressed relative to band density of tissue from control animals (injected with PBS) run on the same blot (therefore, control value = 1.0). Mice were injected with solutions as described in Fig. 3 legend. Data for mice injected with PBS + PEG were virtually identical to data for control mice injected with PBS (data not shown). Values are means ± SE; $n = 4–10$ for each group. *$P <$ 0.05 vs. control.

do possess a gas phase. This is because subjecting particles to hydrostatic pressure would cause a physical distortion that would not occur if they are fluid-filled. If just fluid-filled, MPs would be virtually incompressible. In that case, pressurization to 790 kPa would have the same effect on all molecules in each particle. No physical distortion would be anticipated, and 790 kPa should result in a rather nominal perturbation of particle constituents. That is, the influence of hydrostatic pressure on molecules is dependent on the volume change of a reaction: the rate of a reaction is enhanced if the volume change is negative and inhibited if the volume change is positive. Hydrostatic pressures in hundreds of MPa, not kPa, are required for an effect on protein conformation (9, 16). While MPs are complex protein-lipid structures, pressures far higher than applied in our study are necessary to change physical protein-lipid bilayer characteristics, and hydrostatic pressure may even offer a stabilizing force (11, 22).

The changes in surface protein pattern among the various particle preparations used for injections once again speak to the dynamic nature of MPs. They also complicate interpretation of the pathological effects associated with injecting *type a* vs. *type b* or *c* particles into naive mice. Only *type a* particles caused intravascular neutrophil activation, neutrophil adherence to the vascular wall, caspase-3 activation, and increased vascular permeability. Hydrostatic recompression decreased the number of >1-μm-diameter annexin V particles in *type b* preparations, and PEG emulsified >90% of all the particles. In addition to particle size and gross number, surface protein pattern on *type a* particles may also play a role in proinflammatory effects. In our previous study, however, we noted that MPs expressing CD41 and CD66b were closely associated with development of vascular injuries (23). Given that MPs expressing CD41 and CD66b were more numerous following exposures to hydrostatic pressure (Table 4), they would not be expected to exhibit a decreased propensity for causing neutrophil activation or perivascular injuries compared with *type a* particles.

We also found marked differences in the surface characteristics of circulating MPs isolated from mice 1 h after *type a* and *b* particle injections (Fig. 7) vs. those found in control mice. In our previous study, we noted that MPs interact and share surface markers (23). There were significant elevations in MPs exhibiting a number of markers, including CD41, CD66b, von Willebrand factor, glycophorin A, and tissue factor, from mice injected with *type a* or *b* particles. In fact, there were few differences in the surface markers of circulating MPs from mice injected with these two types of particles. Injections of PEG-treated MPs (*type c*) caused some perturbations in circulating MP surface protein expression, but the results were not significantly different from markers expressed on MPs from control mice injected with PBS.

Annexin V-positive particle retention in blood. In addition to differences in size distribution, surface marker expression pattern, and propensity for causing inflammatory vascular injuries between standard annexin V-positive particles (*type a*) and those subjected to hydrostatic recompression (*type b*), there were also substantial differences in the rate at which they were cleared from the circulation. For example, mice injected with *type a* particles received 6.2×10^6 particles (200 μl × 30,790 particles/μl; Table 3), and 1 h later the number in the circulation was ~8,300/μl (Fig. 6). With the assumption that the average 20-g mouse has a plasma volume of ~980 μl (1), the total count was $\sim 8.1 \times 10^6$ particles. This number would

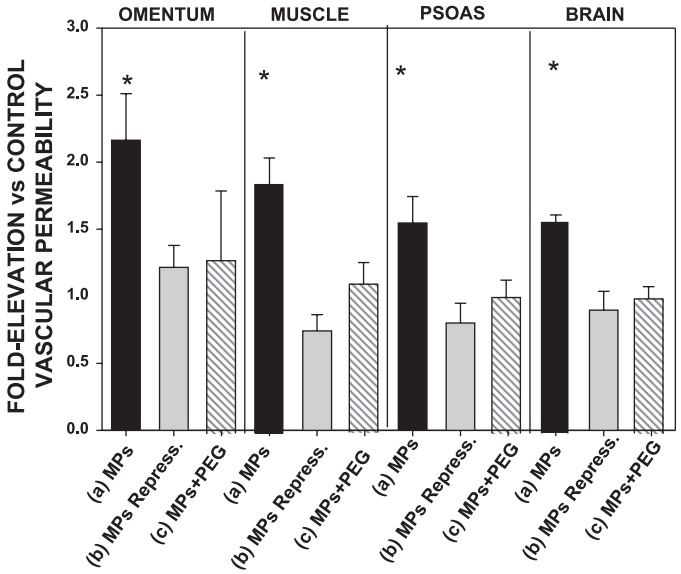

Fig. 5. Rhodamine-labeled dextran uptake, measured as leakage of lysine-fixable rhodamine-conjugated 2×10^6 Da dextran, in mice injected with solutions as described in Fig. 3 legend. Values reflect ratio of fluorescence/mg protein in homogenates from injected mice to that in homogenates from control mice injected with the same lot of rhodamine-dextran and run on the same day. Data for mice injected with PBS + PEG were virtually identical to data for control mice injected with PBS (data not shown). Values are means ± SE; n = 4–10 for each group. *$P < 0.05$ vs. control.

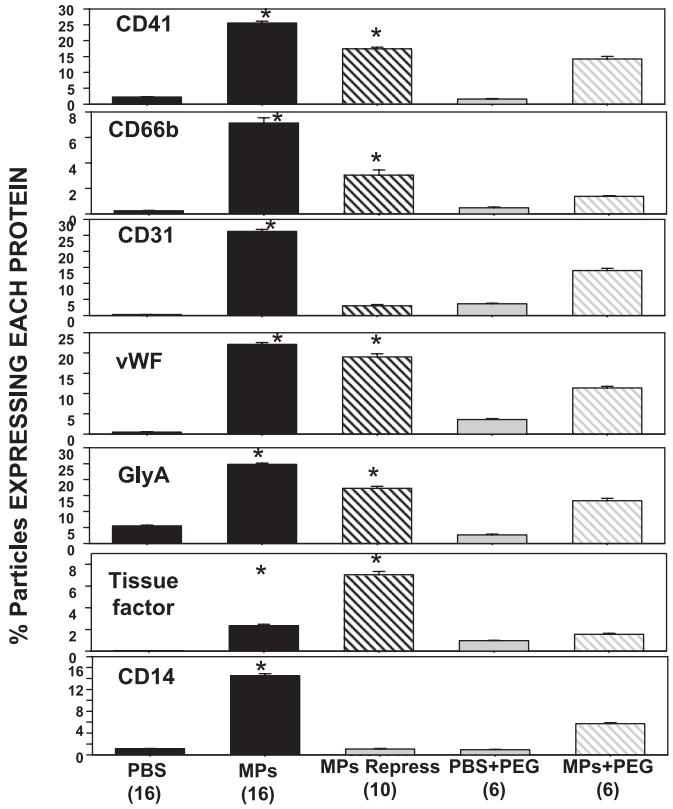

Fig. 7. Proteins expressed on the surface of MPs: fractions of MPs expressing the platelet-specific CD41, the neutrophil protein CD66b, CD31 (platelet endothelial cell adhesion molecule), von Willebrand factor (vWF), the erythrocyte-specific protein glycophorin A (GlyA), tissue factor, and the common leukocyte antigen CD14. Values are means ± SE for number of animals shown (in parentheses) for each group. *$P < 0.05$ vs. control (PBS).

be expected, given that the average mouse has ~2,000 MPs/μl before any manipulations, or a total of 2×10^6 MPs (control mice in this report and as reported in our previous study) (23); that is, $6.2 \times 10^6 + 2 \times 10^6 = 8.2 \times 10^6$ particles in these mice. This suggests that there was virtually no clearance of particles in the 1 h following injection. In contrast, mice injected with particles subjected to hydrostatic pressure (*type b*) received ~8.4×10^6 particles (42,119/μl × 200 μl; Table 3), and 1 h later the number in the circulation was ~3.9×10^6 (3,900/μl × 980 μl; Fig. 6). Again with the assumption that the mice had ~2×10^6 MPs prior to the injection, ~62% {100 × [1 − (3.9/8.4 + 2)]} were cleared from the circulation in the 1 h after injection. We recognize, however, that our interpretation may be somewhat simplistic. That is, because MPs are proinflammatory (at least, *type a*), it is possible that some of the MPs seen after injection of *type a* particles are due to production of new particles from pathological intravascular events that do not occur with *type b* and *c* MPs because of their smaller size and/or different surface marker expression pattern.

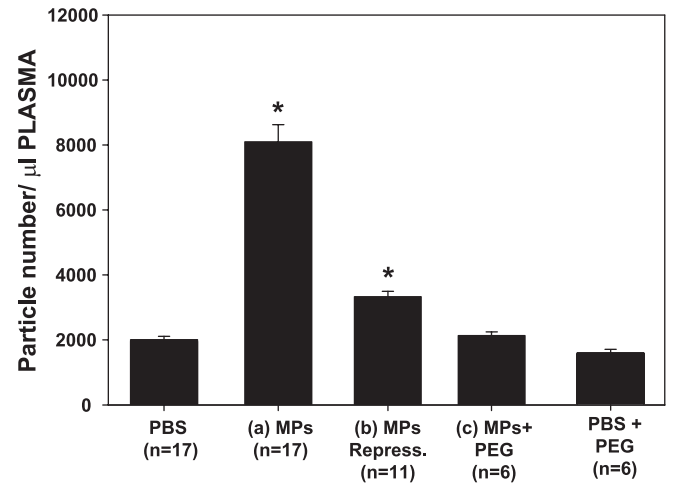

Fig. 6. Circulating annexin V-positive particles in mice killed 1 h after injections with various preparations as described in Fig. 3 legend. Values are means ± SE for number of animals shown for each group (n). *$P < 0.05$ vs. control (PBS). Values for MPs Repress and MPs are significantly different from each other.

In summary, we conclude from this study that injection of annexin V-positive particles from decompressed mice will recapitulate the pathophysiological vascular changes observed in decompressed mice (23). Particle injections will cause

Table 4. *Surface proteins expressed on MPs used for intravenous injections*

Surface Protein	Standard (n = 17)	Recompressed (n = 11)	PEG-Incubated (n = 6)
CD41	25.7 ± 0.4*	44.6 ± 2.5*	16.2 ± 0.9*
CD66b	5.5 ± 0.2	29.6 ± 0.8*	3.3 ± 0.6
CD31	24.3 ± 0.6*	56.1 ± 2.4*	12.9 ± 0.6*
von Willebrand factor	20.8 ± 0.5*	50.0 ± 1.8*	11.6 ± 0.4*
Glycophorin A	22.0 ± 0.3*	47.8 ± 1.7*	12.3 ± 0.3*
Tissue factor	2.1 ± 0.1*	28.3 ± 1.7*	0.6 ± 0.1*
CD14	9.8 ± 0.3*	30.7 ± 1.5*	5.8 ± 0.3*

Values are means ± SE, expressed as percentage of total; n, number of animals. MPs, microparticles. *$P < 0.05$ vs. the other 2 samples in the same row.

intravascular neutrophil activation, neutrophil adherence to the vascular wall, caspase-3 activation, and increased vascular permeability. Furthermore, we find that the pathological impact of injected annexin V-positive particles can be profoundly altered with ex vivo manipulations. Results indicate that a certain particle size distribution and/or surface protein pattern is required to initiate proinflammatory vascular injuries.

Our results provide additional insight into decompression pathophysiology; therefore, they are relevant for SCUBA diving, high-altitude aviation, and space exploration. Questions persist regarding the mechanism for MP enlargement postdecompression, differences in inflammatory responses caused by particles manipulated ex vivo in different ways, and the kinetics of particle clearance. Further work is required to address these questions and also to ascertain whether elevations in the total number and diameters of circulating annexin V-positive particles occur in humans subjected to decompression stresses.

GRANTS

This work was supported by a grant from the US Office of Naval Research. G. Uzun was supported by a grant from the Scientific and Technological Research Council of Turkey.

DISCLOSURES

No conflicts of interest, financial or otherwise, are declared by the authors.

REFERENCES

1. **Altman PL, Dittmer DS.** *Biology Databook.* Washington, DC: FASEB, 1964, p. 264.
2. **Brubakk AO, Duplancic D, Valic Z, Palada I, Obad A, Bakovic D, Wisloff U, Dujic Z.** A single air dive reduces arterial endothelial function. *J Physiol* 566: 901–906, 2005.
3. **Connor DE, Exner T, Ma DD, Joseph JE.** The majority of circulating platelet-derived microparticles fail to bind annexin V, lack phospholipid-dependent procoagulant activity and demonstrate greater expression of glycoprotein Ib. *Thromb Haemost* 103: 1044–1052, 2010.
4. **Eftedal OS, Lydersen S, Brubakk AO.** The relationship between venous gas bubbles and adverse effects of decompression after air dives. *Undersea Hyperb Med* 34: 99–105, 2007.
5. **Enjeti AK, Lincz LF, Seldon M.** Detection and measurement of microparticles: an evolving research tool for vascular biology. *Semin Thromb Hemost* 33: 771–779, 2007.
6. **Enjeti AK, Lincz LF, Seldon M.** Microparticles in health and disease. *Semin Thromb Hemost* 34: 683–692, 2008.
7. **Fox FE, Herzfeld KF.** Gas bubbles with organic skins as cavitation nuclei. *J Acoust Soc Am* 26: 984–989, 1954.
8. **Hugel B, Martinez MC, Kunzelmann C, Freyssinet JM.** Membrane microparticles: two sides of the coin. *Physiology* 20: 22–27, 2005.
9. **Hummer G, Garde S, Garcia AE, Paulaitis ME.** The pressure dependence of hydrophobic interactions is consistent with the observed pressure denaturation of proteins. *Proc Natl Acad Sci USA* 95: 1552–1555, 1998.
10. **Jy W, Mao WW, Horstman L, Tao J, Ahn YS.** Platelet microparticles bind, activate and aggregate neutrophils in vitro. *Blood Cells Mol Dis* 21: 217–231, 1995.
11. **Kangur L, Timpmann K, Freiberg A.** Stability of integral membrane proteins under high hydrostatic pressure: the LH2 and LH3 antenna pigment-protein complexes from photosynthetic bacteria. *J Phys Chem B* 112: 7948–7955, 2008.
12. **Lo SC, Hung CH, Lin DT, Peng HC, Huang TF.** Involvement of platelet glycoprotein Ib in platelet microparticle mediated neutrophil activation. *J Biomed Sci* 13: 787–796, 2006.
13. **Madden LA, Chrismas BC, Mellor D, Vince RV, Midgley AW, McNaughton LR, Atkins SL, Laden G.** Endothelial function and stress response after simulated dives to 10 msw breathing air or oxygen. *Aviat Space Environ Med* 81: 41–51, 2010.
14. **Martin JD, Thom SR.** Vascular leukocyte sequestration in decompression sickness and prophylactic hyperbaric oxygen therapy in rats. *Aviat Space Environ Med* 73: 565–569, 2002.
15. **Mesri M, Altieru DC.** Leukocyte microparticles stimulate endothelial cell cytokine release and tissue factor induction in a JNK1 signaling pathway. *J Biol Chem* 274: 23111–23118, 1999.
16. **Mozhaev VV, Heremans K, Frank J, Masson P, Balny C.** High pressure effects on protein structure and function. *Proteins* 24: 81–91, 1996.
17. **Nossum V, Hjelde A, Brubakk AO.** Small amounts of venous gas embolism cause delayed impairment of endothelial function and increase polymorphonuclear neutrophil infiltration. *Eur J Appl Physiol* 86: 209–214, 2002.
18. **Nossum V, Koteng S, Brubakk AO.** Endothelial damage by bubbles in the pulmonary artery of the pig. *Undersea Hyperb Med* 26: 1–8, 1999.
19. **Olszanski R, Radziwon P, Baj Z, Kaczmarek P, Giedrojc J, Galar M, Kloczko J.** Changes in the extrinsic and intrinsic coagulation pathways in humans after decompression following saturation diving. *Blood Coagul Fibrinolysis* 12: 269–274, 2001.
20. **Philp RB, Ackles KN, Inwood MJ, Livingstone SD, Achimastos A, Binns-Smith M, Radomski MW.** Changes in the hemostatic system and in blood and urine chemistry of human subjects following decompression from a hyperbaric environment. *Aerospace Med* 43: 498–505, 1972.
21. **Pirro M, Schillaci G, Bagaglia F, Menecali C, Paltriccia R, Mannarino MR, Capanni M, Velardi A, Mannarino E.** Microparticles derived from endothelial progenitor cells in patients at different cardiovascular risk. *Atherosclerosis* 197: 757–767, 2008.
22. **Schuster B, Sleytr UB, Diederich A, Bahr G, Winterhalter M.** Probing the stability of S-layer-supported planar lipid membranes. *Eur Biophys J* 28: 583–590, 1999.
23. **Thom SR, Yang M, Bhopale VM, Huang S, Milovanova TN.** Microparticles initiate decompression-induced neutrophil activation and subsequent vascular injuries. *J Appl Physiol* 110: 340–351, 2011.
24. **Vince RV, McNaughton LR, Taylor L, Midgley AW, Laden G, Madden LA.** Release of VCAM-1 associated endothelial microparticles following simulated SCUBA dives. *Eur J Appl Physiol* 105: 507–513, 2009.
25. **Yount DE.** On the elastic properties of the interfaces that stabilize gas cavitation nuclei. *J Colloid Interface Sci* 193: 50–59, 1997.
26. **Yount DE, Kunkle TD, D'Arrigo JS.** Stabilization of gas cavitation nuclei by surface active compounds. *Aviat Space Environ Med* 48: 185–189, 1977.